Research in Marine Sciences
Volume 5, Issue 2, 2020
Pages 681 - 698

Upwelling in the northwest Sabah during the northeast monsoon and its relation with El–Niño

Muhammad Naim Satar[1], Mohd Fadzil Akhir[2,*], Poh Heng Kok[2], and Nurul Rabitah Daud[3]

[1]Institute of Oceanography and Environment, Universiti Malaysia Terengganu, 21030 Kuala Nerus, Terengganu, Malaysia

[2]Associate Professor, Institute of Oceanography and Environment, Universiti Malaysia Terengganu, 21030 Kuala Nerus, Terengganu, Malaysia

[3]Faculty of Civil Engineering, Universiti Teknologi MARA, 40450 Shah Alam, Selangor, Malaysia

Received: 2020-02-11 *Accepted: 2020-05-18*

Abstract

This study analyzes the characteristics of upwelling events during the northeast monsoon, as well as El-Niño impacts towards upwelling in the northwest Sabah, which is located in southern part of the South China Sea by combining remote sensing, reanalysis, and modeling data. The data used in this study obtained from Moderate Resolution Imaging Spectroradiometer (MODIS) Aqua satellite for the sea surface temperature (SST) and chlorophyll *a* concentration data, Hybrid Coordinate Ocean Model (HYCOM) for the vertical cross section of temperature and salinity data, and European Centre for Medium-range Weather Forecast (ECMWF) Interim Reanalysis (ERA-Interim) for the wind data, as well as Ekman transport and Ekman pumping analysis during December to April 2003-2016. The monthly mean of the climatological data were analyzed and the results showed that the MODIS-Aqua satellite indicates the presence of cooler sea surface temperature (SST) and higher chlorophyll-*a* concentration along the inshore region of northwest Sabah during the northeast monsoon, indicating the existence of upwelling. Cross-sectional temperature profiles obtained from the HYCOM further confirmed the existence of upwelling as the thermohaline was uplifted from the deeper layer and reached the surface during the northeast monsoon. Ekman transport and Ekman pumping derived from the ECMWF showed an upwelling favorable condition during the northeast monsoon. Comparison between climatological data and El-Niño year in 2016 represented that El-Niño events somehow increase the upwelling intensity due to the intensification of Ekman transport and Ekman pumping.

Keywords: Upwelling; South China Sea; Northwest Sabah; Northeast monsoon; El-Niño.

* Corresponding Author’s email: mfadzil@umt.edu.my

1. Introduction

Upwelling is a well-known phenomenon in ocean studies as it can enhance the primary productivity of the coastal area, making the upwelling region served as one of the most productive regions (Anderson and Lucas, 2003). Wind-driven upwelling is the best-known types of upwelling and it is mainly formed by two processes, i.e. Ekman transport and Ekman pumping (Pickett and Paduan, 2003; Kok *et. al*, 2017).

Sabah is located in the southeastern part of the South China Sea (SCS) and it is in the East Malaysia, to be a part of Borneo Island (Figure 1). The East-Asian Monsoon predominantly influences the SCS, i.e. the southwest and northeast monsoons (Wyrtki, 1961). During the southwest monsoon from June until August, the SCS dominated by southwesterly winds whereas during the northeast monsoon from December until February, the wind reversed its direction to northeasterly (Wang *et al.*, 2013). Upwelling in the SCS started to be observed since 1950. Then, a rigorous study done by many researchers in the continental shelf of SCS where the northern SCS had been predominant focal region for the upwelling events compared to other places such as Southern Vietnam and Luzon Strait (Ndah *et al.*, 2016). In the southwest monsoon, upwelling can be found in the South Vietnam (Xie *et al.*, 2003), Hainan Island, Taiwan Strait (Hu *et al.*, 2003), and the East Coast of Peninsular Malaysia (ECPM) (Akhir *et al.*, 2015; Zainol and Akhir, 2016; Kok *et al.*, 2017). As for the northeast monsoon, to date, only two upwelling areas had been analyzed, which are in the Luzon area and the northwest Sabah. Nonetheless, there are very few reports published on upwelling in the northwest Sabah, hence many features yet to be discovered.

Son *et al.* (2005) mentioned the presence of upwelling in the northwest Sabah; where they used Pacific Fisheries Environmental Laboratory (PFEL) live access from NOAA website and found that positive wind stress curl at the northwest Sabah induces upwelling. Besides, many studies pointed out that there is a potential of the existence of upwelling since algal blooms and higher chlorophyll-*a* (Chl *a*) are common (Knee *et al*., 2006; Abbas *et al.*, 2012; Abdul-Hadi *et al.*, 2013). Yan *et al.* (2015) are the first researchers that successfully give a good understanding of upwelling in the northwest Sabah by using combining several datasets from satellite data, climatological temperature, salinity fields, and reanalysis data.

El Niño Southern Oscillation (ENSO) starts in equatorial Pacific and occurs within 2-7 years, and is one of the random events that can modulate many atmospheric and oceanic processes such as in the SCS. For example, the 1982-1983 El-Niño weakened surface circulation and caused higher Sea Surface Temperature (SST) in the whole SCS (Chao *et al*., 1996). In 1997-1998 El-Niño events, the sea surface height over the SCS deep basin was lower than usual (Ho *et al*., 2000). For the upwelling process, Kuo *et al.* (2003) showed that the 1997 El Niño events strengthen the monsoon winds, enhancing the summer upwelling in southern Vietnam and induced the upwelling center to move southward from May to August 1997. Jing *et al.* (2011) also indicated that the intensification of summer upwelling in the northern South China Sea (Taiwan Strait and Hainan Island) during 1997 El-Niño due to the presence of anticyclonic atmospheric circulation anomaly over the SCS and northwest Pacific. Another study by Daud *et al.* (2019) showed during 2009-

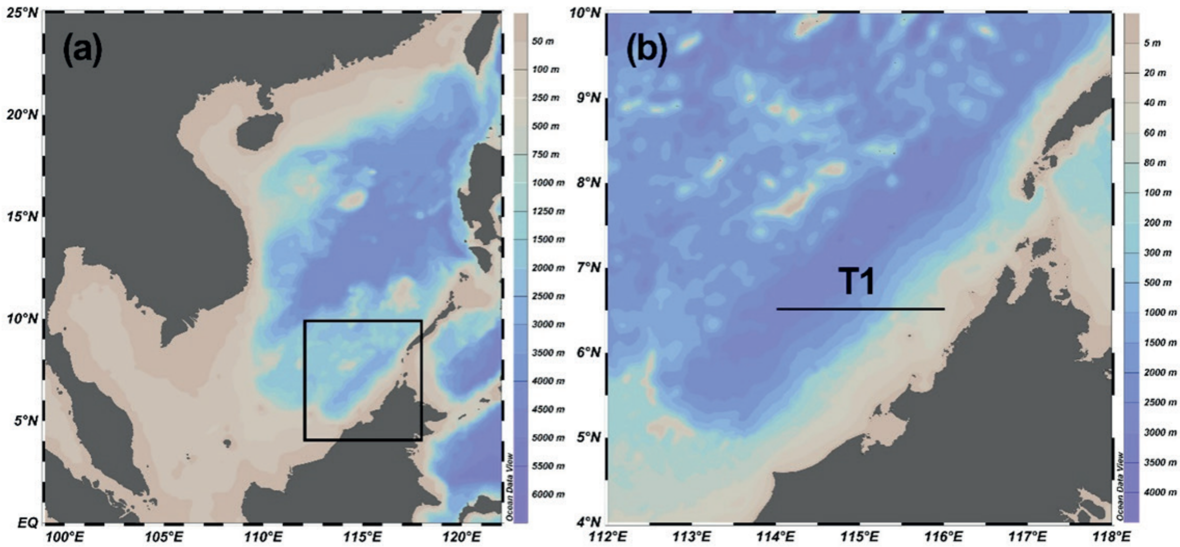

Figure 1. Map and bathymetry of southern part of the South China Sea (a), and the study area Sabah (b). The transect T1 is for HYCOM temperature profile. The bathymetry of the area is higher than 2000m [Image adapted from Ocean Data View]

2010 El Niño, the El-Niño events resulted in the favorable condition for the stratification of the water column, thus weakened the upwelling in the ECPM. For Sabah area, Yan *et al.* (2015) said that the strengthened of upwelling is due to the presence of anticyclonic wind with higher magnitude that increases the intensity of the favorable upwelling wind in the study area during El-Niño years, but their study did not show a monthly variation of wind analysis during the El-Niño event.

Therefore, this study intends to extend the knowledge by studying the characteristics of the upwelling in the northwest Sabah by using several combinations of monthly climatology data obtained from Moderate-resolution Imaging Spectrometers (MODIS) sensor, Hybrid Coordinate Ocean Model (HYCOM), European Centre Medium-range Weather Forecast (ECMWF). We also compared the results obtained from climatology data and the 2015-2016 El Niño events to analyze the El-Niño impacts towards upwelling events in the northwest Sabah.

2. Materials and methods

2.1. Remote Sensing Data

Monthly climatology satellite-derived SST and Chl-*a* concentration data obtained from MODIS instrument aboard the Aqua satellite (MODIS-Aqua) and the data is available in https://oceancolor.gsfc.nasa.gov/. Aqua satellite was launched in 2002, viewing the entire Earth's surface every two days, acquiring data in 36 spectral bands. The domain of the study area is illustrated in Figure 1.

In this study, data of 14 years (2003-2016) of MODIS-Aqua Level-3 monthly SST climatology, 11µ band, nighttime with 4km spatial resolution were used which includes Chl *a*, Level-3 monthly climatology from 2003-2016, OCI Algorithm, with 4km resolution.

Furthermore, the monthly data (January-March) in 2016 for SST data was used to be compared with the climatology data for the El-Niño study.

2.2. Modeling output

Modeling outputs for cross-sectional temperature and salinity profile were obtained from HYCOM, https://www.hycom.org/ for 2012-2013 during the northeast monsoon. HYCOM is a multi-institutional effort that aims to develop and evaluate the data-assimilative hybrid isopycnal-sigma-pressure (generalized) coordinate ocean model. The computations of this data are carried out on a Mercator grid between 78 °S and ٤٧ °N (١/١٢° equatorial resolution), and a bipolar patch is used for regions north of 47 °N. The horizontal dimensions of the global grid are ٤٥٠٠ × 3298 grid points resulting in about 7 km spacing on average, and the total 32 vertical layers been produced. The data assimilation is done by the Navy Coupled Ocean Data Assimilation (NCODA) system (Cummings, 2005). In this study the NCODA uses the model forecast as a first guess in a Multivariate Optimal Interpolation (MVOI) scheme and assimilates available satellite altimeter observations (along-track) obtained via the NAVOCEANO Altimeter Data Fusion Center) satellite and in-situ SST as well as available in-situ vertical temperature and salinity profiles from XBTs, ARGO floats, and moored buoys (GOFS 3.1: 41-layer HYCOM + NCODA Global 1/12° Reanalysis, n.d).

2.3. Wind Data

The monthly 10-m zonal and meridional wind data from the year 2003 to 2016 and wind at 850hpa with 0.25° × 0.25º resolution obtained from ECMWF, Interim Reanalysis (ERA-Interim) website, https://www.ecmwf.int/. Calculation of Ekman transport at each grid point on the basis of wind products obtained from ERA-Interim by using the following equation following the methods used by Kok *et al.* (2017):

$$Q_x = \frac{\tau_y}{\rho_w f} \qquad Q_y = -\frac{\tau_x}{\rho_w f} \tag{1}$$

where, is the wind stress, = 1025 kg m^{-3} is the density of seawater, and = 2Ω sin θ is the Coriolis parameter (Ω = 7.292 × 10^{-5} rad/s is the Earth's angular velocity, and θ is the latitude). The x and y subscripts refer to the zonal and meridional wind components of Ekman transport, respectively. is calculated as follows:

$$\tau_x = \rho_a C_d ({W_x}^2 + {W_y}^2)^{\frac{1}{2}} W_x$$
$$\tau_y = \rho_a C_d ({W_x}^2 + {W_y}^2)^{\frac{1}{2}} W_y \tag{2}$$

where, P_a = 1.22 kg/m^3 is the density of air, C_d = 1.3 × 10^{-3} is the constant dimensionless drag coefficient, and W is the wind speed at 10 m.

For the Ekman pumping (EP), the calculation was made for each grid point by using a formula as follows:

$$EP = \frac{\text{curl}\,(\tau)}{\rho_w f} \tag{3}$$

where, P_W = 1025 kg/m^3 and curl (τ) is the wind stress curl, which is calculated as follows:

$$\text{curl}\,(\tau) = \frac{\partial \tau_y}{\partial_x} - \frac{\partial \tau_x}{\partial_y} \tag{4}$$

3. Results and Discussion

3.1. MODIS-Aqua Data

Figure 2 shows the spatio-temporal of monthly SST climatology for 2003-2016 from December to April. In December, the cooler SST remains absent, but the SST for almost the whole study area started to cool down to ~28 °C. In January, the SST with 27 °C started to appear

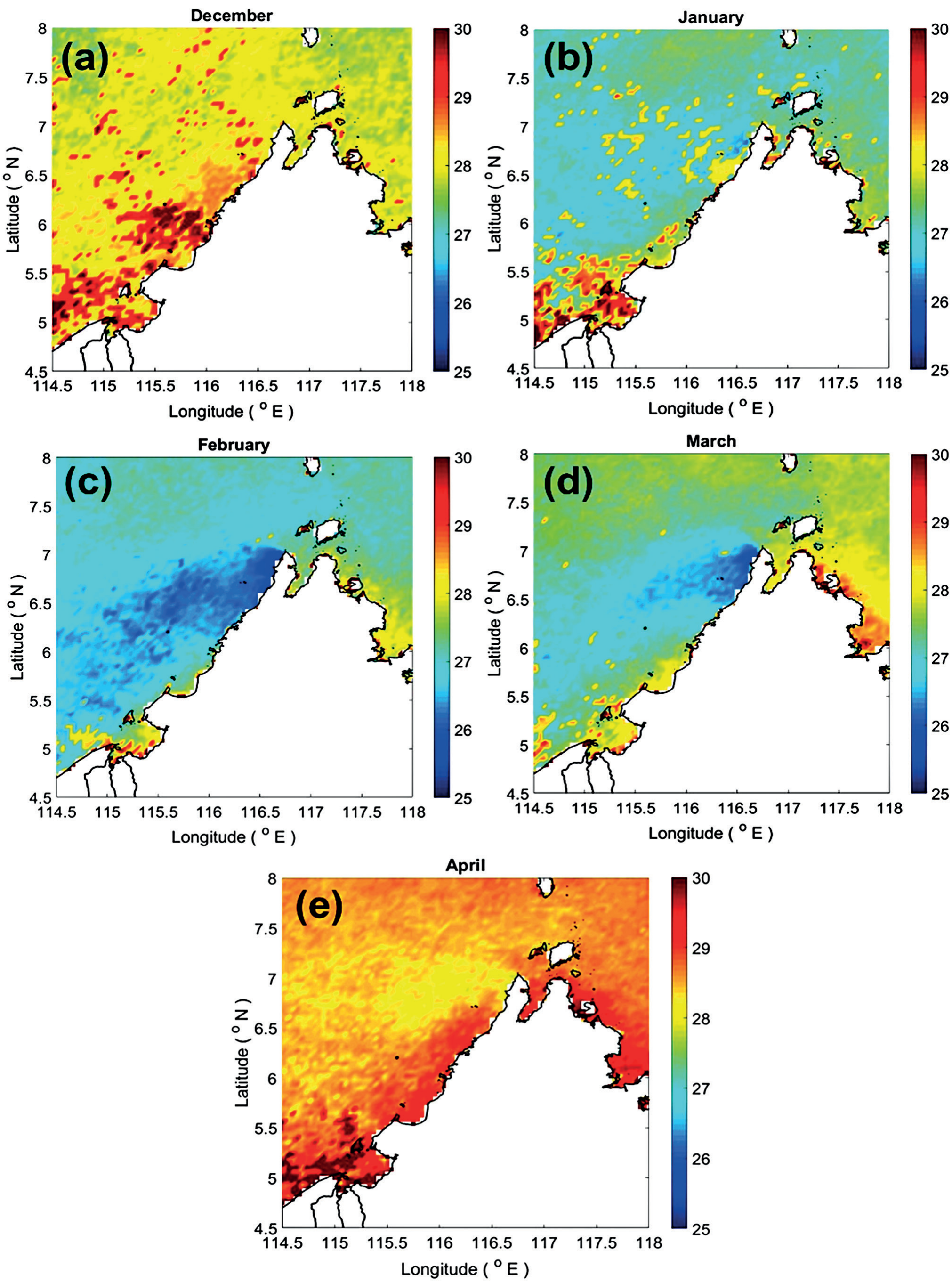

Figure 2. Monthly climatology of SST (unit: °C) for 2003-2016, (a) December, (b) January, (c) February, (d) March, and (e) April. Note that the cloud cover from January 2011 data causes the presence of patches of slightly higher SST in January.

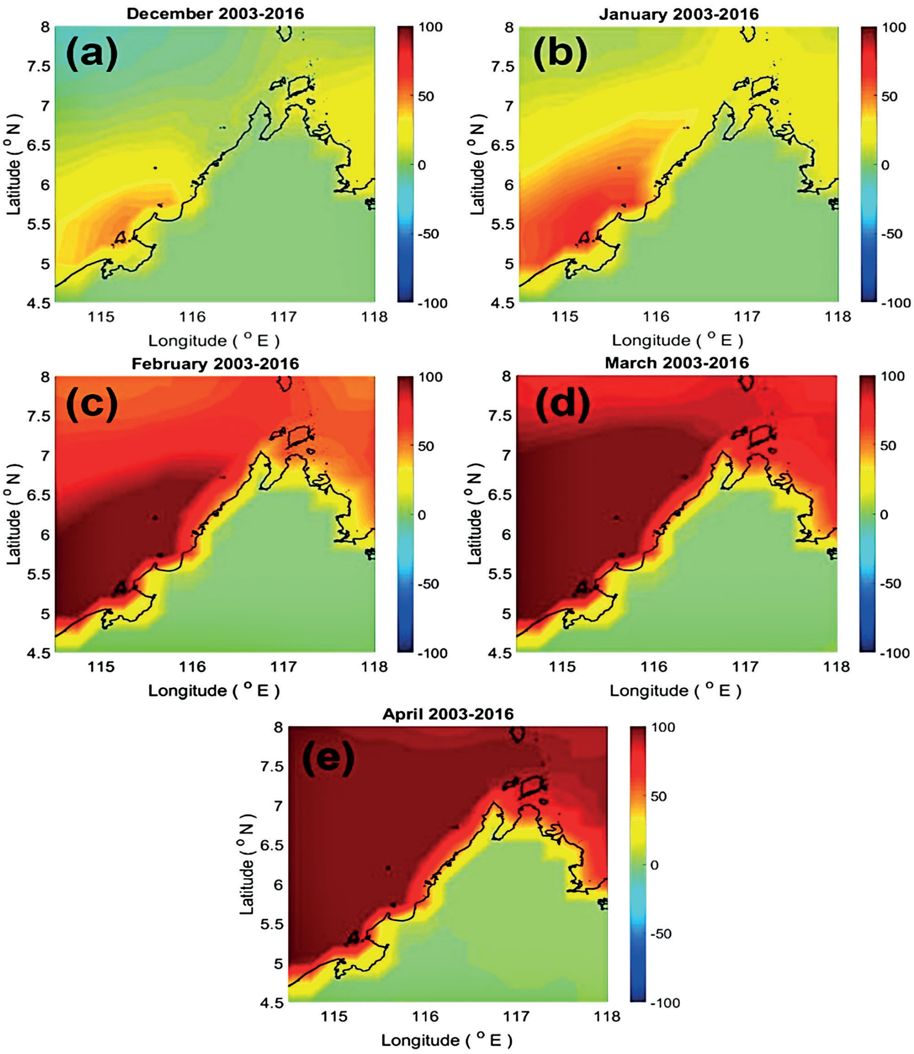

Figure 3. Monthly climatology of net heat flux (unit: mW/m^2) from 2003-2016, (a) December, (b) January, (c) February, (d) March, and (e) April [Image adapted from ERA5]

and dominates the inshore area, and then these cooler SST continues to drop off until 26 °C and almost completely dominates the inshore area of northwest Sabah in February. These cooler 26 °C SST spatial areas started to decrease in March as the SST started to increase. Finally, the cooler 26 °C SST fully disappeared in April, leaving only the small area of SST with 27 °C in the northern part of the study area.

Since the heat flux also might affect the SST, thus the monthly climatology mean of net heat flux from 2003-2016 during northeast season, taken from ERA5 data were plotted in Figure 3, that clearly shows the high positive heat flux (heat absorbed) present in the study area especially during starting from January and keeps increasing until March. This indicates that the heat flux does not really contribute to the low SST as the high heat flux has been recorded.

Figure 4 indicates the spatio-temporal of monthly climatology Chl-*a* concentration. A higher concentration of Chl-*a* only appeared at the southern coast of northwest Sabah, which might occur due to the high nutrients input

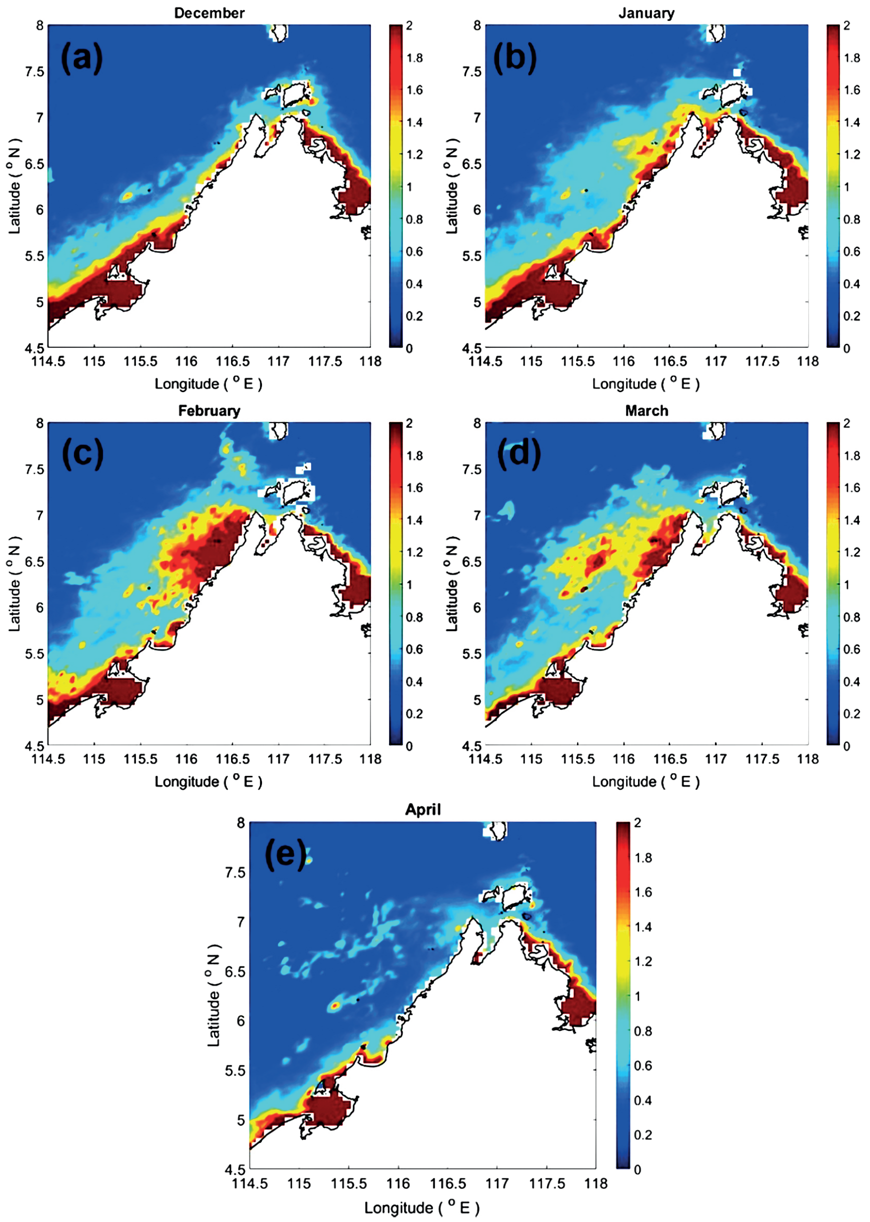

Figure 4. Monthly climatology Chl-*a* concentration (unit: mg/m^3) for 2013-2016, (a) December, (b) January, (c) February, (d) March, and (e) April

from the local river (Sun, 2017). Then, the higher Chl-*a* concentration started to appear at the coastal area of the northwest Sabah in January, where the concentration reaches up to $2mg/m^3$. In February and March, this higher Chl-*a* concentration keep on increasing spread towards the offshore region and cover almost the whole northwest Sabah before started to disappear in April. As we observed, these trend of high Chl-*a* concentration are well coincided with the lower SST that appear in the study area for each of the months.

SST and Chl-*a* concentration are two elements that widely used as the indicators for an upwelling because upwelling usually brings cooler and higher nutrients water from the deeper layer to the surface layer of the ocean (Bakun *et al.*, 2015). This cooler water reduces the SST value in the study area, and higher nutrients input will lead to high primary productivity, which increased the Chl-*a* concentration. Thus, from the 14 years of climatology data that were shown in Figures 2 and 4, we observed an obvious change in SST and Chl-*a* during northeast monsoon season where lower SST and higher Chl-*a* coincided with each other for each month, indicating the occurrence of upwelling event.

3.2. HYCOM modeling output

The HYCOM modeling outputs from December 2012 to April 2013 were analyzed to obtain more understanding on upwelling event in the study area. This period (2012-2013) was chosen for the HYCOM data because during this period there are no ENSO events that might interrupt with the upwelling occurrences. From the Figure 5, isotherm was uplifted in almost all months but with different temperatures. Isotherm with 27 °C water uplifted during

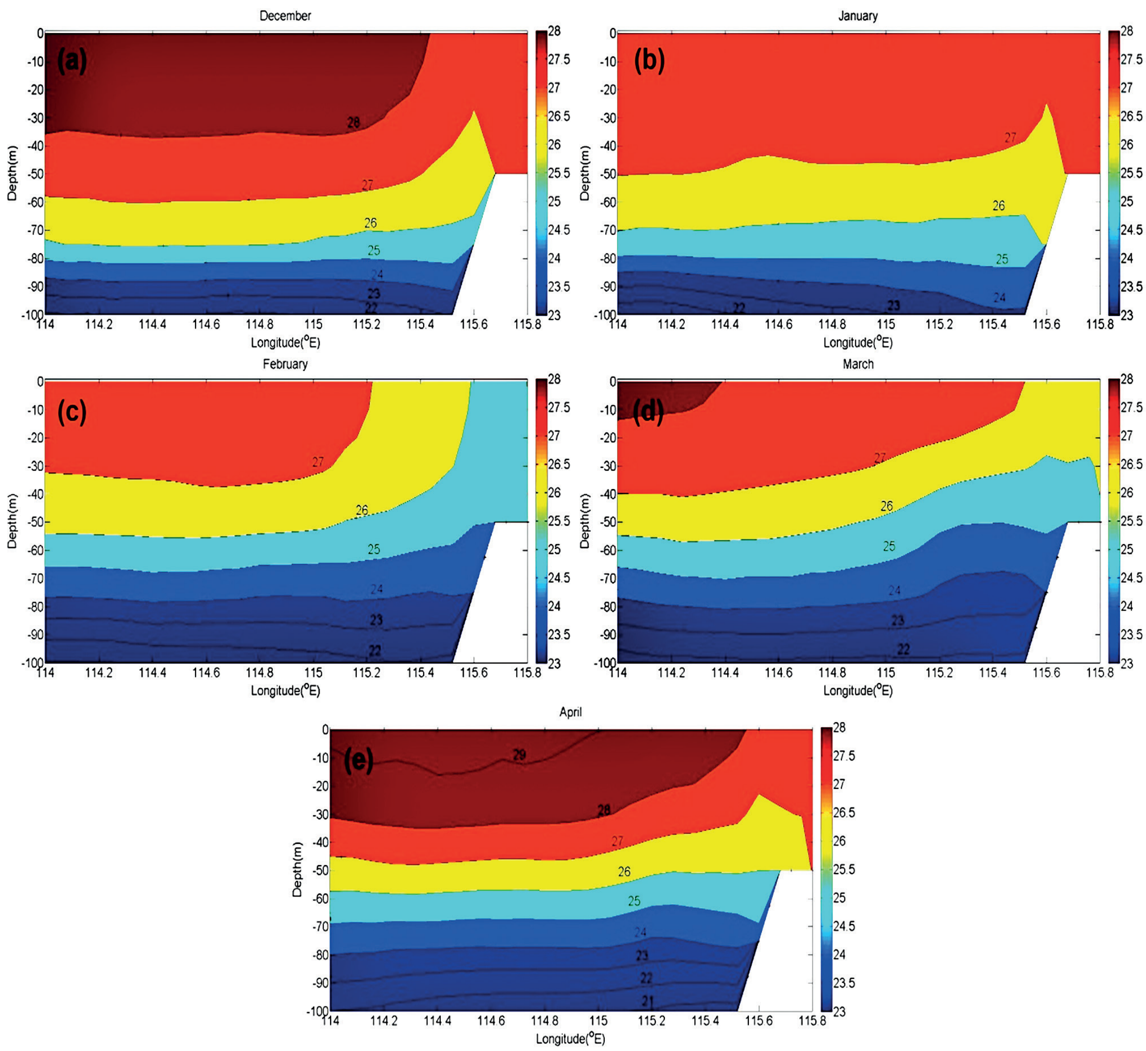

Figure 5. Vertical profile of temperature (unit: °C) from December 2012 to April 2013, (a) December, (b) January, (c) February, (d) March, and (e) April

December 2012 at longitude 115.4 °E from depth of ~35m to the surface. In January, there is no isotherm uplifting observed. However, the upper layer was replaced with slightly cooler water with >27 °C as compared to December. February recorded the lowest temperature of the water, and the 25 °C isotherm was uplifted from depth of ~30m at the (115.2 °E) to the surface. In March, the uplifting of 27 °C isotherm still exists, and finally, in April, isotherm uplifting still exists about 28 °C of the isotherm.

The salinity profile also showed similar trends with the temperature profile in Figure 6. Even though the isohaline uplifting can be observed from month December to February, but the difference salinity value varies in each month. February showed a strong isohaline uplifting, where water with 33.8psu uplifted from depth of ~80m and reaches to the surface. The salinity value does not drop when entering March, and it keeps on increasing from March to April. This might occur due to the higher temperature that leads to higher evaporation and less precipitation in March and April, which are the end of the northeast monsoon season.

This analysis of HYCOM from month

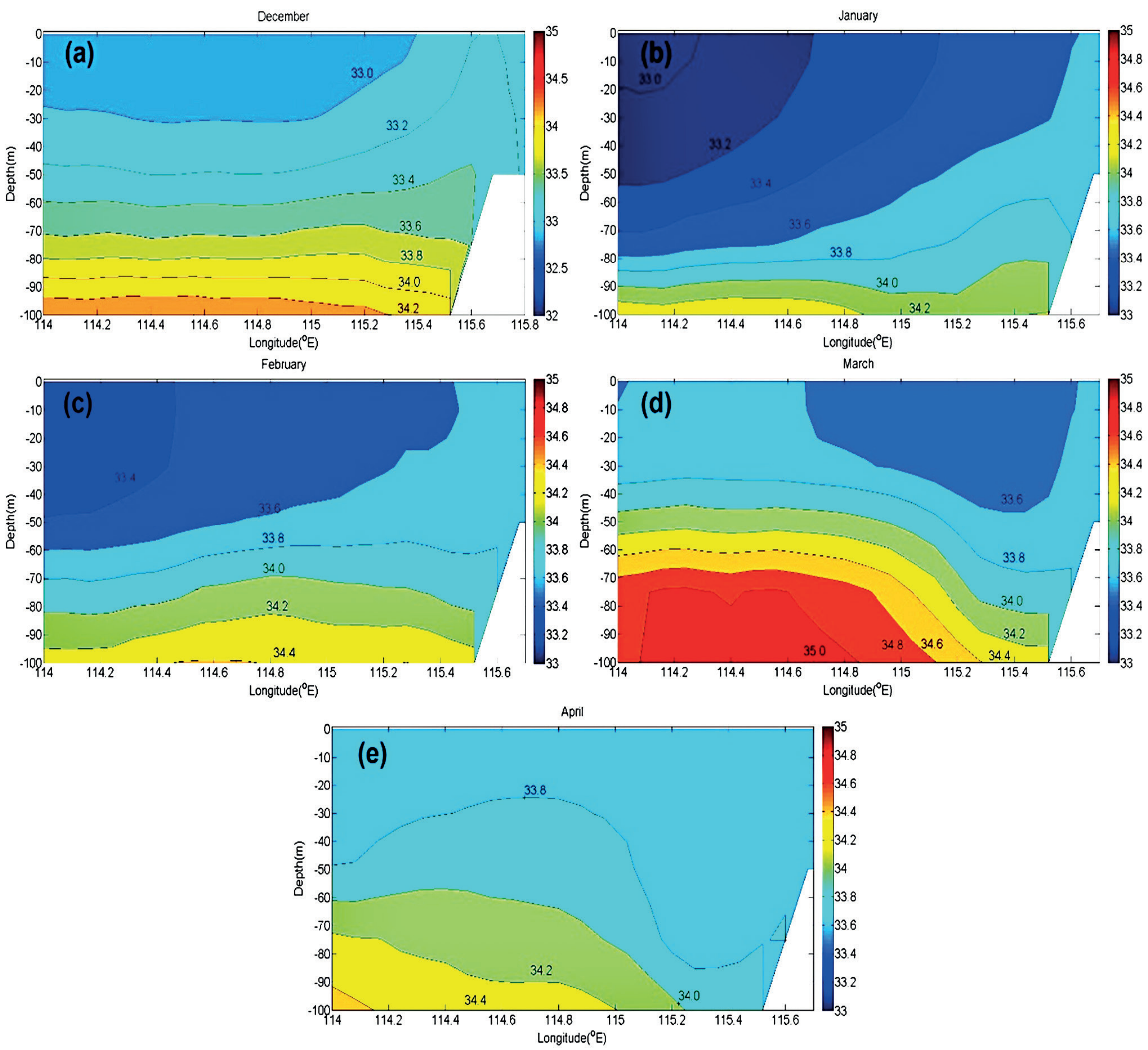

Figure 6. Vertical profile of salinity (unit: psu) from December to April 2012-2013, (a) December, (b) January, (c) February, (d) March, and (e) April

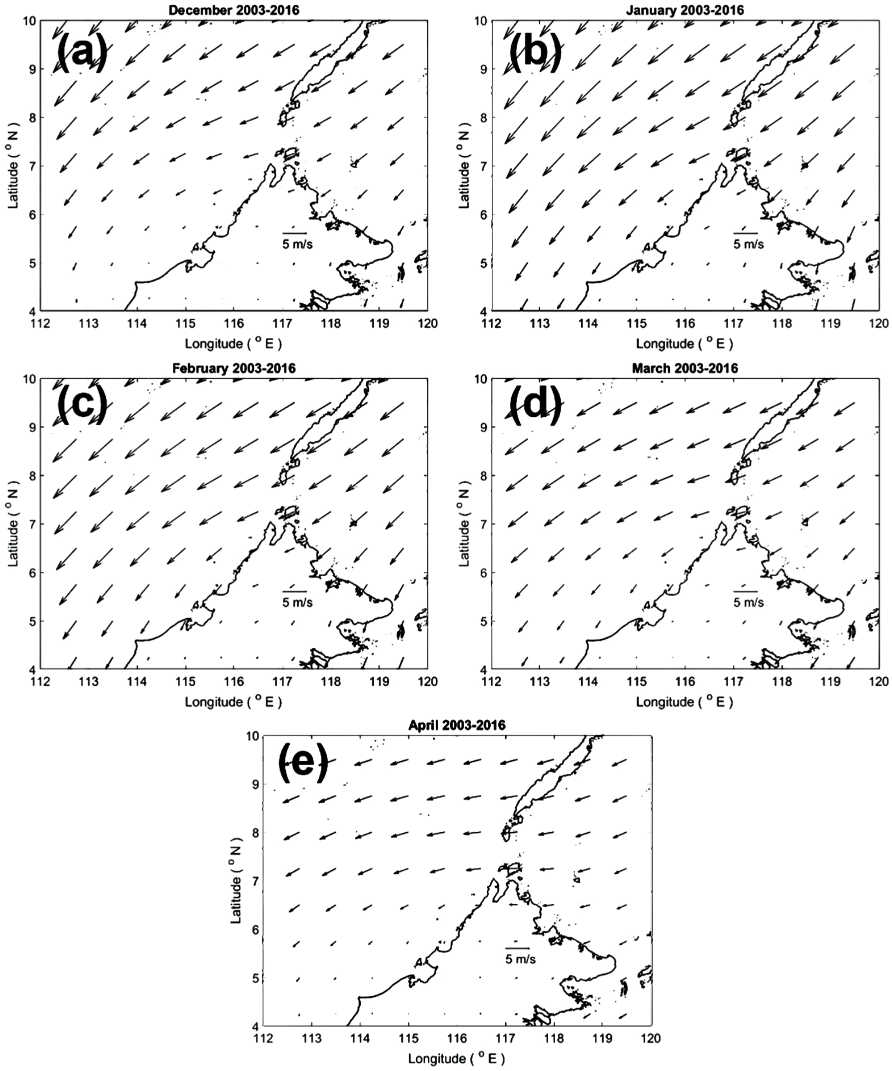

Figure 7. Monthly climatology of surface wind vectors and magnitude (unit: m/s) for 2003 – 2016, (a) December, (b) January, (c) February, (d) March, and (e) April

December 2012 to April 2013 revealed the thermohaline was uplifted during the northeast monsoon, where the isotherm and isohaline uplifting has been traditionally referred as an indicator of upwelling. Besides, we also found that during the month of February, the lowest value of water temperature (25 °C) along with salinity of 33.8psu moves upward and reaches to the surface, again almost similar with the results obtained by SST data where the lowest value of SST were recorded in February.

3.3. Wind Data

Wind acts as a main factor in upwelling events. Therefore, to analyze the wind effects towards upwelling in the study area, monthly climatology wind in northwest Sabah during 2003-2016 are plotted in Figure 7, which shows strong northeasterly wind blows during the northeast monsoon season.

Apart from the wind direction, wind speed also plays important roles in upwelling where stronger winds lead to stronger Ekman transport, which results in stronger upwelling intensity. However, even though wind speed in March decreased, Chl-*a* (Figure 3) observed to be slightly maintained in March. This might occur due to the high nutrients input from the nearby river which pumps nutrients into the sea (Abbas *et al.*, 2012). These two factors (wind speed and its direction) are very crucial to determine the upwelling. It can be observed in January and February (Figure 7), where a strong northeasterly wind leads to strong Ekman transport, that during March and April, the Ekman transport started to be weakened due to change in direction and lower wind speed in these two months.

When the wind blows parallel to the coastline, the Ekman transport will be deflected to the right of the wind direction in the Northern Hemisphere due to the Coriolis Effect, resulting

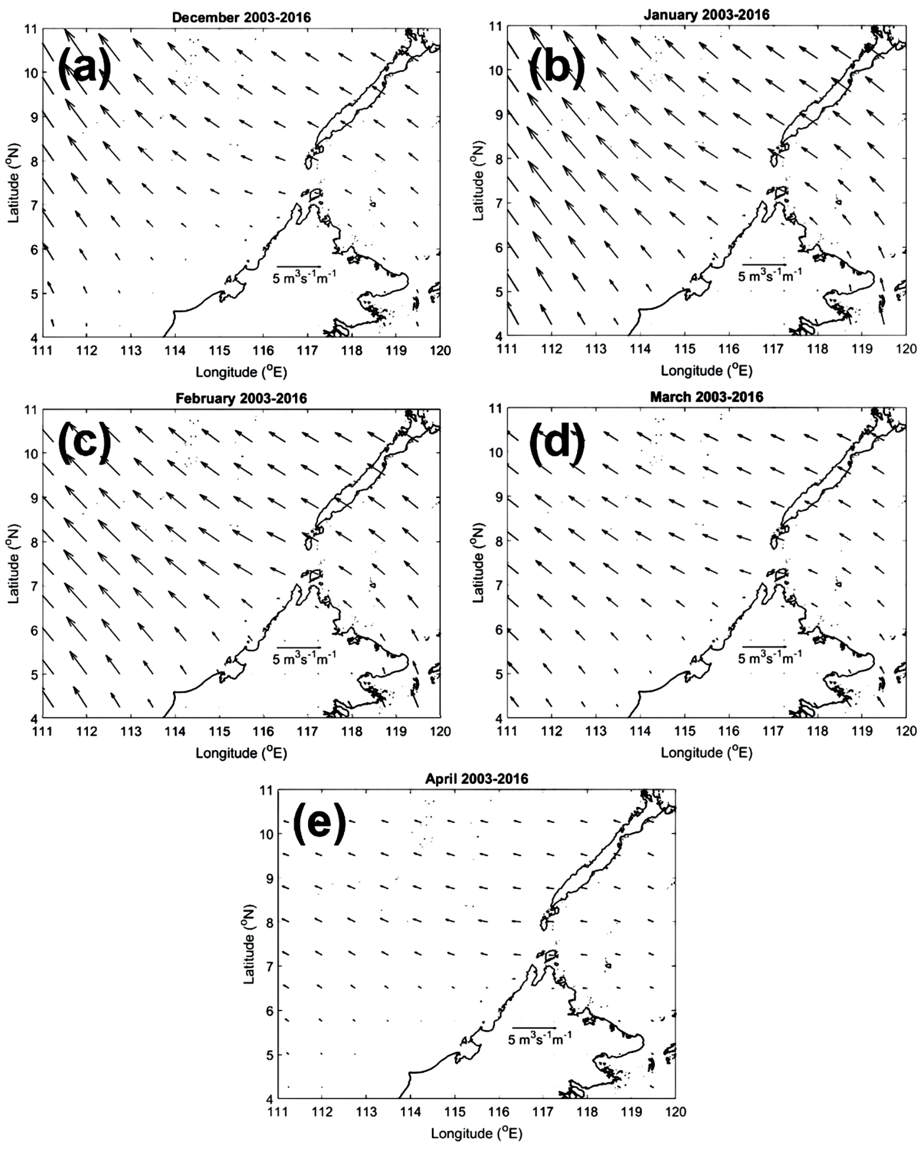

Figure 8. Ekman transport monthly climatology (unit: $m^3/s.m$) from December to April 2003-2016, (a) December, (b) January, (c) February, (d) March, and (e) April

in the net transport of water been deflected 90° to the right which moves away from the coast (Ekman, 1905). From Figure 8, offshore Ekman transport appeared to be present in the study area, favorable for upwelling. Again, the months January and February showed almost similar strength in Ekman transport, indicating that the upwelling are strong during these two months. The Ekman transport intensity started to decrease during March and almost to disappear in April.

Ekman pumping is also another factor that can lead to the upwelling formation, where the positive wind stress curl generates surface divergence, which is upwelling favorable that allows the water rises up from bottom to the surface (Kok *et al.*, 2015; Kok *et al.*, 2017).

Figure 9 shows the positive Ekman pumping started to develop in the study area during December at the northern tip of Sabah, and it is observed that the presence of positive Ekman pumping appeared in the small area at the inshore region of northwest Sabah. During January, the positive Ekman pumping started to increase its intensity and covered almost the whole northwest Sabah area, and it

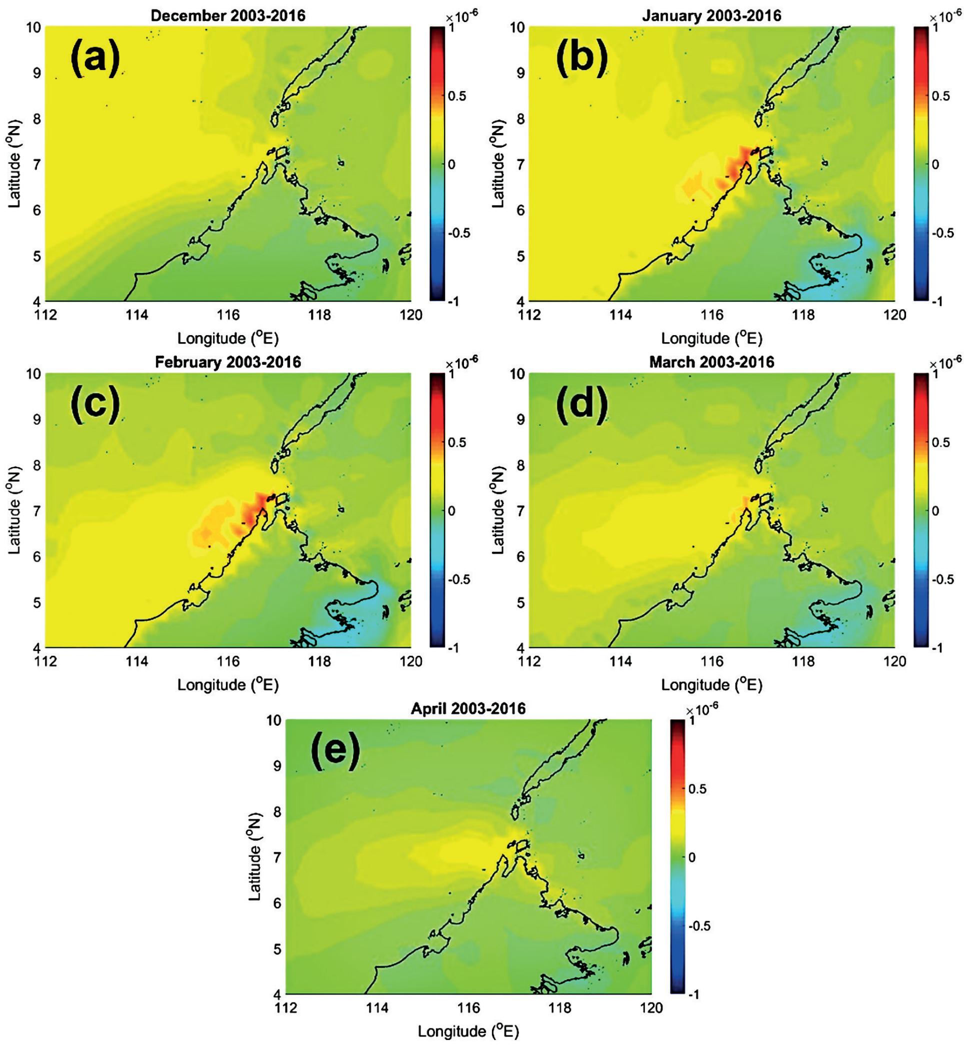

Figure 9. Ekman pumping monthly climatology (unit: m/s) for 2003-2016, (a) December, (b) January, (c) February, (d) March, and (e) April

keeps increasing in February before declining in March and again almost is disappeared in April. These two Ekman proved that upwelling events are present in northwest Sabah as both of the Ekman transport and Ekman pumping favorable for upwelling.

3.4. El-Niño impacts toward upwelling

As we mentioned earlier, El-Niño have significant impacts on the upwelling. Thus, to know the El-Niño effects on the upwelling in northwest Sabah, the data comparison between climatology data and El-Niño year during 2016 is conducted.

Firstly, we compare the monthly SST data for both climatology and El-Niño years during 2016. Figure 10 indicates that the trend of upwelling is the same, but upwelling during El-Niño 2016 are intensified, where the lower SST with 26 °C is present in January, compared to the climatological data where the cool SST just

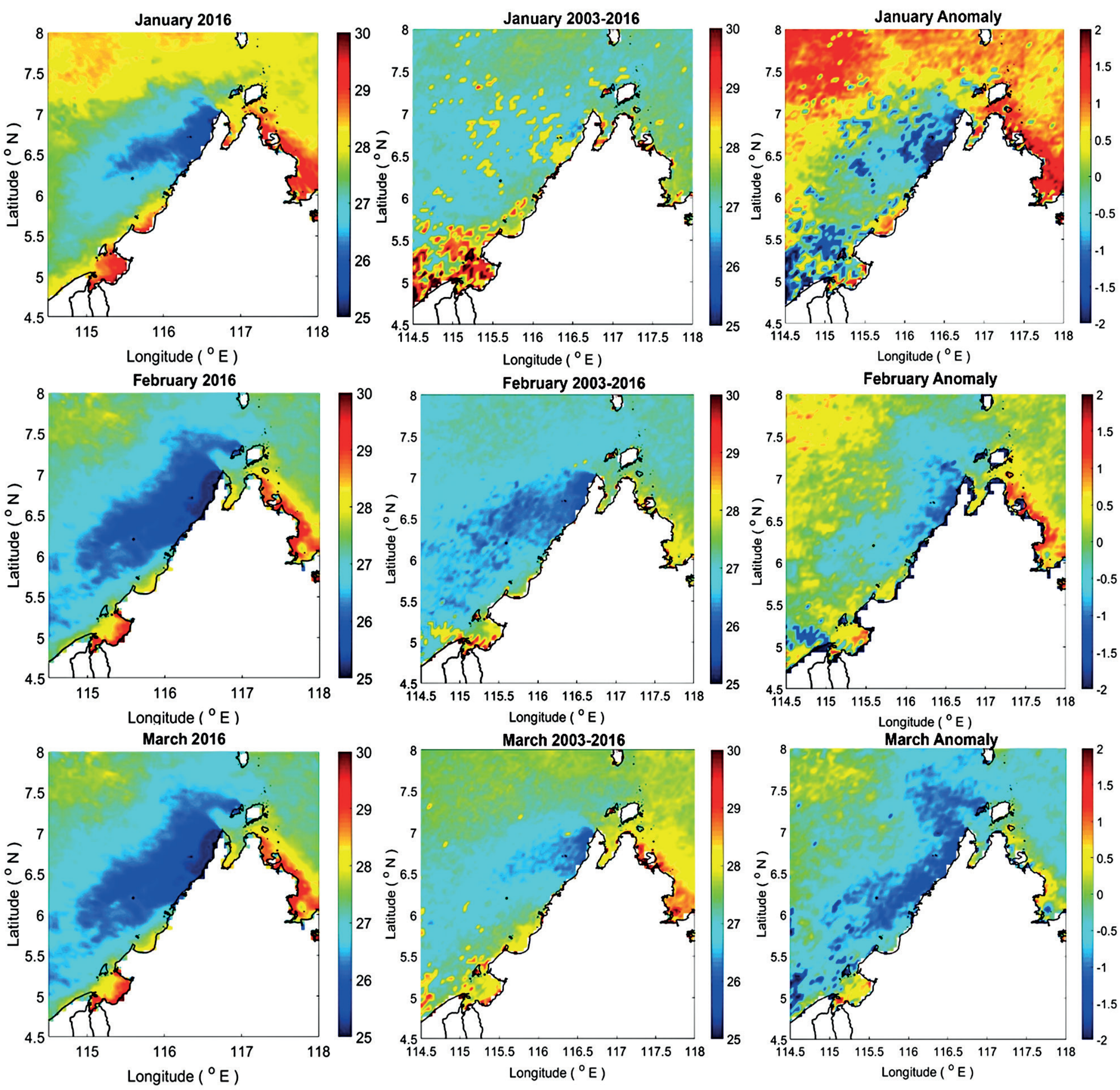

Figure 10. Monthly SST (unit: °C) for 2016 (left), climatology (middle), and anomaly (right)

started to develop during this month. Lower SST values in comparison with the climatological data have also been recorded for the two other months (February and March) during this ENSO year. The anomaly map (data from January 2016 minus climatology data) further proves that the SST during El-Niño 2016 is much lower than the climatological data.

As the wind plays an important role in upwelling, we try to analyze the wind data for both data. Based on the results obtained, it showed that surface wind (Figure 11) during El-Niño years in 2016 is observed to be stronger than the climatological data for the whole three months based on the anomaly data. This stronger wind in 2016 might leads to stronger upwelling events in the study area.

Since the wind data is not enough to explain the intensification of upwelling, thus we do further analysis of the wind to observe the Ekman transport and Ekman pumping. For the Ekman transport analysis, Figure 12 indicates that the Ekman transport is observed to be quite stronger in terms of magnitude during El-Niño in 2016 compared to climatology data for the whole three months especially during January

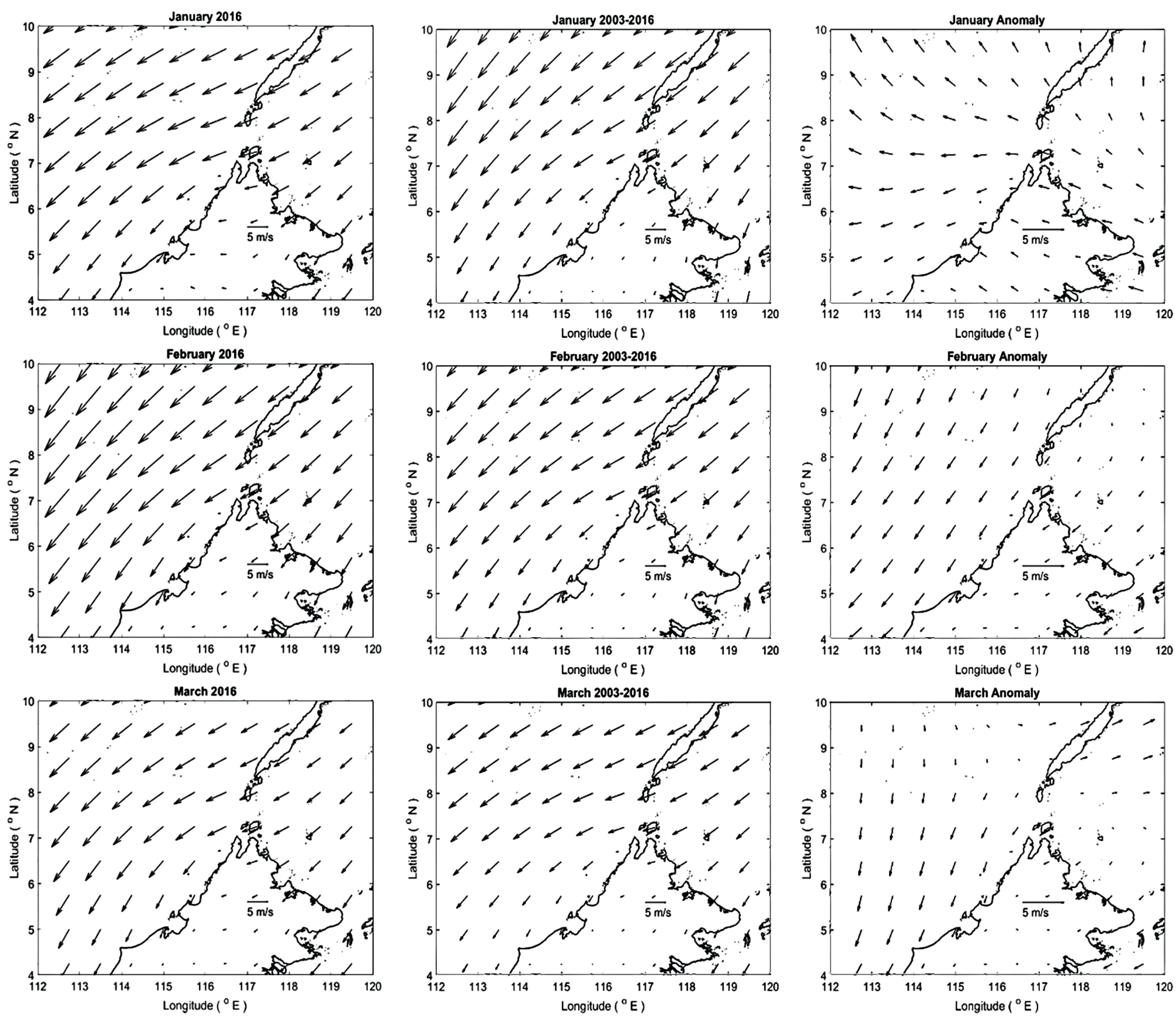

Figure 11. Surface wind vector and magnitude (unit: m/s) for the year 2016 (left) and climatology 2003-2016 (middle), and anomaly (right)

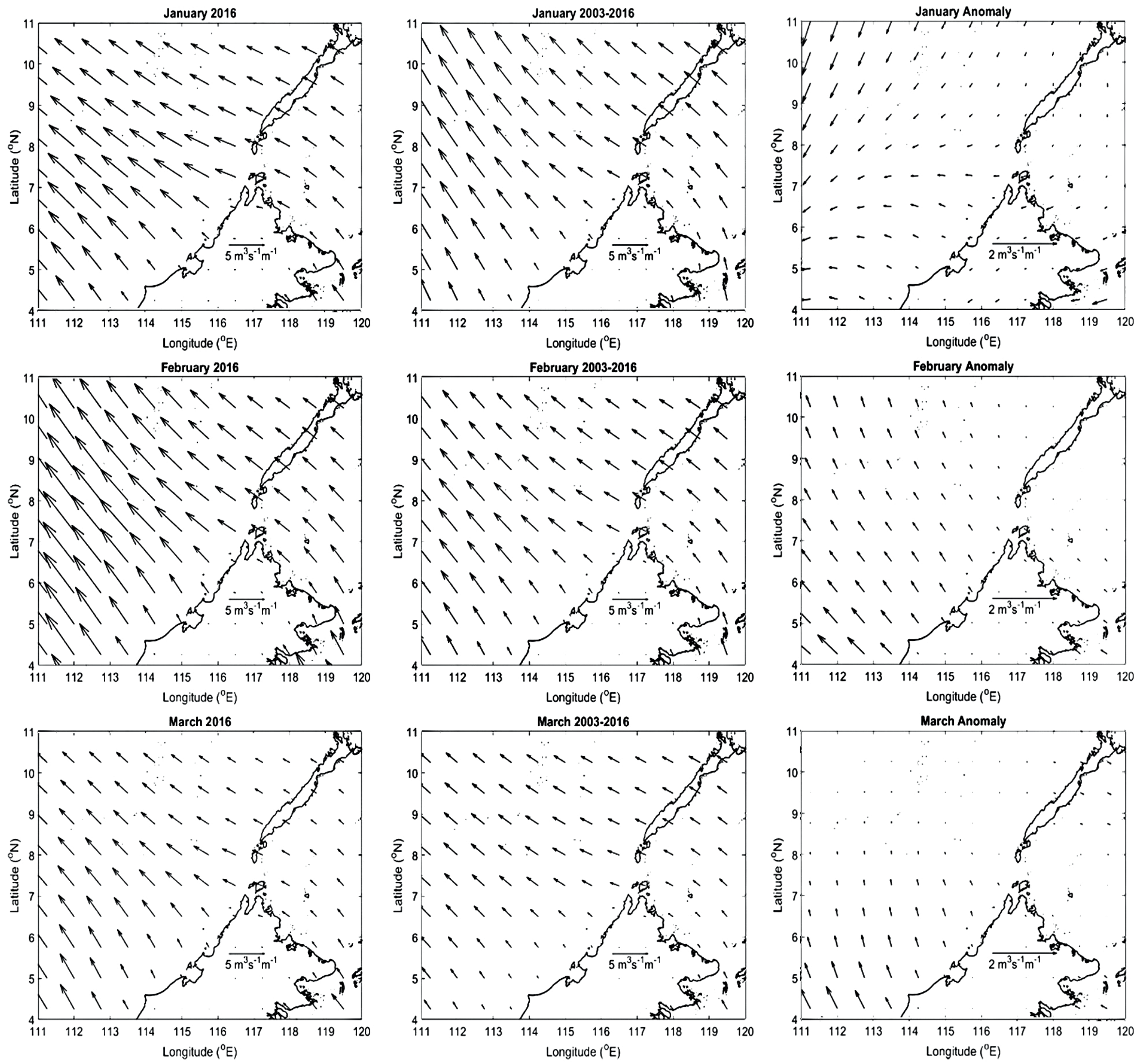

Figure 12. Ekman transport (unit: $m^3/s \cdot m$) for year 2016 (left), climatology data 2003-2016 (middle), and anomaly data (right)

and February where a longer arrow formed in 2016, as well as anomaly data. This further proves that the upwelling was intensified during El-Niño 2016.

For the Ekman pumping analysis (Figure 13), a very distinctive result obtained where the very strong positive wind stress curl that formed in the year 2016 for the whole three months compared to a low intensity of positive wind stress curl in the climatological data. This indicates that during El-Niño years, positive Ekman pumping wind are intensified at the study area, thus generates stronger upwelling events during these El-Niño years. Strengthen of Ekman transport and Ekman pumping might be due to the anticyclonic wind circulation anomaly over the SCS that develop during the El-Niño years (Jing *et al.*, 2011). This anticyclonic wind anomaly is generated by Atmosphere Bridge which behaves as northeasterly and positive wind stress curl anomaly at the study area, and so enhances the upwelling event (Yan *et al.*, 2015).

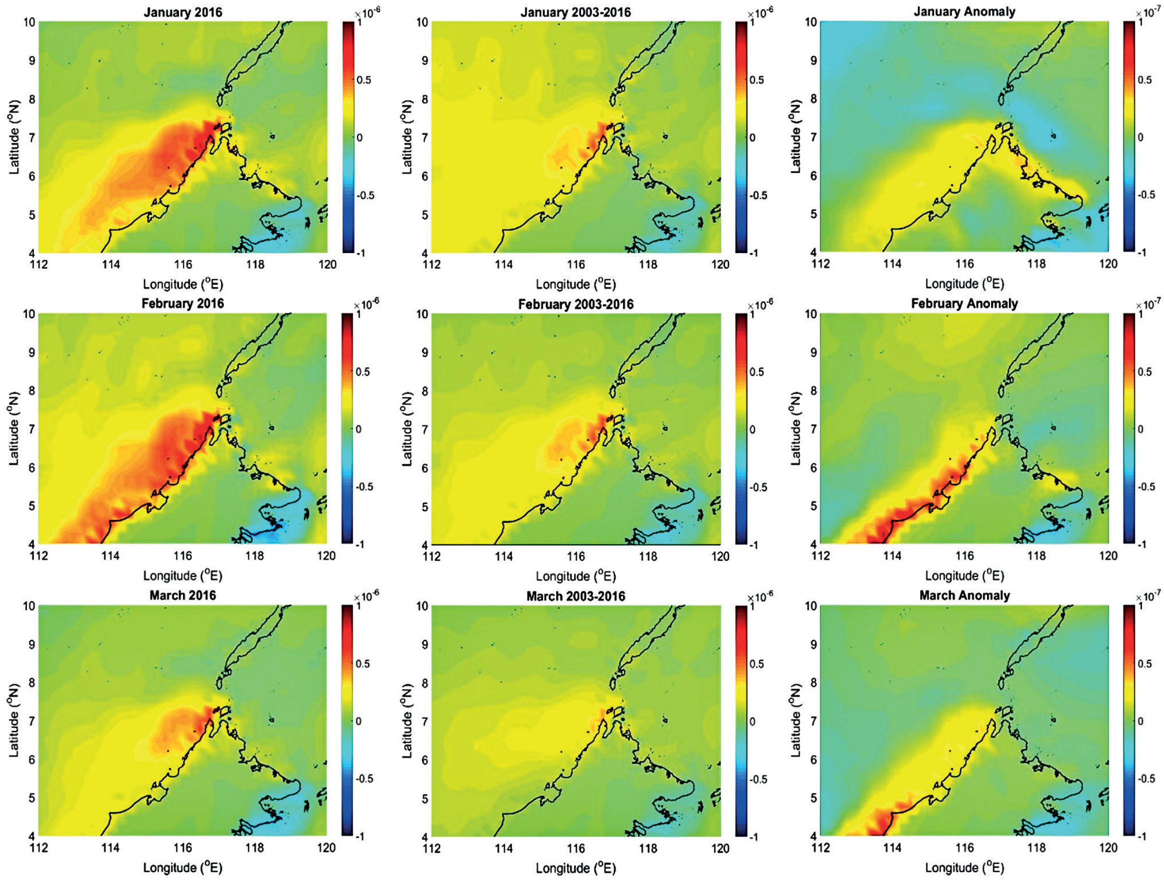

Figure 13. Ekman pumping (unit: m/s) in the study area in 2016 (left), climatology 2003-2016 (middle), and anomaly (right)

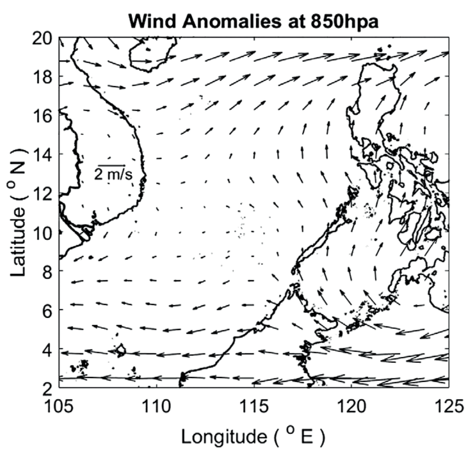

Figure 14. Wind anomalies vector and magnitude (unit: m/s) at 850hpa

Analyzing wind anomalies at 850-hpa (January-March) shows clearer vision on how the upwelling is intensified during the year. Wind at 850hpa is considered as the most natural wind, as the wind is not disrupted by any structures such as buildings, mountains, etc. Based on Figure 14, it is observable that below 6 ºN there are strong easterly wind, but to the north the wind curl northward, where this wind might be one of the reason that enhance the upwelling system by providing more positive wind stress curl leading to positive Ekman pumping based on what Yan *et al.* (2015) mentioned in their study.

Conclusion

In this study, upwelling in the northwest Sabah has been revealed using a combination of remote sensing, modeling output, and reanalysis data. Monthly variation of SST and Chl-*a* showed that upwelling occurred during the northeast monsoon, starting from December, reached to maximum intensity in February, and started to decrease in March. A strong northeasterly wind blows parallel to the shoreline of northwest Sabah, resulting in offshore Ekman transport. Besides, positive Ekman pumping also formed due to wind divergence that presence in the study area, responsible for upwelling. El-Niño events give significant impacts on ocean processes as well as on upwelling event in the northwest Sabah. Upwelling in northwest Sabah showed stronger intensity during El-Niño year in 2016 compared to the climatology data, as lower SST values and higher wind intensity lead to higher Ekman transport and Ekman pumping.

Acknowledgment

This study was supported by the Ministry of Higher Education on both FRGS and Higher Institution Centre of Excellence (HICoE) Grant awarded to the Institute of Oceanography and Environment (INOS), Universiti Malaysia Terengganu (UMT), International Collaboration Fund (ICF) provided by Ministry of Science, Technology and Innovation (MOSTI), Malaysia. All authors have no financial or other conflicts of interest.

References

Abbas, A. A., Mansor, S. B., Pradhan, B., and Tan, C. K. 2012. Spatial and seasonal variability of Chlorophyll-a and associated oceanographic events in Sabah water. Proceedings of the 2nd International Workshop on Earth Observation and Remote Sensing Applications, EORSA 2012, (June): 215–219. https://doi.org/10.1109/ EORSA.2012.6261168

Abdul-Hadi, A., Mansor, S., Pradhan, B., and Tan, C. K. 2013. Seasonal variability of chlorophyll-a and oceanographic conditions in Sabah waters in relation to Asian monsoon - A remote sensing study. Environmental Monitoring and Assessment, 185(5): 3977–3991. https://doi.org/10.1007/s10661-012-2843-2

Akhir, M. F., Daryabor, F., Husain, M. L. Tangang, F., and Qiao, F. 2015. Evidence of Upwelling along Peninsular Malaysia during Southwest Monsoon. Open Journal of Marine Science, 5(July): 273–279. https://doi.org/10.4236/ojms.2015.53022

Anderson, T.R., and Lucas, M.I. 2008. Upwelling ecosystems. In: Jorgensen, S.E.; Fath, B., (eds.) Encyclopedia of Ecology. New York, USA: Elsevier Science.

Bakun, A., Black, B. A., Bograd, S. J., Garcia-Reyes, M., Miller, A. J., Rykaczewski, R. R., and Sydeman, W. J. 2015. Anticipated effects of climate change on coastal upwelling ecosystems. Current Climate Change Reports, 1(2): 85-93.

Chao, S. Y., Shaw, P. T., and Wu, S. Y. 1996. El Niño modulation of the South China sea circulation. Progress in Oceanography, 38(1): 51-93.

Ekman, V. W. 1905. On the Influence of Earth's Rotation on Ocean-Currents, 2(11): 1–52.

GOFS 3.1: 41-layer HYCOM + NCODA Global 1/12° Reanalysis (n.d). Retrieved from https://www.hycom.org/dataserver/gofs-3pt1/reanalysis

Ho, C. R., Kuo, N. J., Zheng, Q., and Soong, Y. S. 2000. Dynamically active areas in the South China Sea detected from TOPEX/POSEIDON satellite altimeter data. Remote Sensing of Environment, 71(3): 320-328.

Hu, J., Kawamura, H., Hong, H., and Pan, W. 2003. A review of research on the upwelling in the Taiwan Strait. Bulletin of Marine Science, 73(3): 605-628.

Jing, Z., Qi, Y., and Du, Y. 2011. Upwelling in the continental shelf of northern South China Sea associated with 1997-1998 El Niño. Journal of Geophysical Research: Oceans, 116(C2).

Knee, T. C., Ishizaka, J., Ransi, V., Phuoc, T., Son, H., and et al. 2006. Oceanographic events at northern Borneo and their relationship to harmful algal blooms. International Symposium on Remote Sensing 2006 Pan Ocean Remote Sensing Conference.

Kok, P. H., Akhir, M. F. M., Tangang, F., and Husain, M. L. 2017. Spatiotemporal trends in the southwest monsoon wind-driven upwelling in the southwestern part of the South China Sea. PLoS ONE, 12(2): 1-22. https://doi.org/10.1371/journal.pone.0171979

Kok, P. H., Akhir, M. F., and Tangang, F. T. 2015. Thermal frontal zone along the east coast of Peninsular Malaysia. Continental Shelf Research, 110: 1–15. https://doi.org/10.1016/j.csr.2015.09.010

Ndah, B. N., Becek, K., and Dagar, L. 2016. A Review of Coastal Upwelling Research in the South China Sea: Challenges, Limitations, and Prospects. International Journal of Earth And Atmospheric Science, 3(4): 63–72.

Pickett, M. H., and Paduan, J. D. 2003. Ekman transport and pumping in the California Current based on the U.S. Navy's high-resolution atmospheric model (COAMPS). Journal of Geophysical Research, 108(C10): 3327. https://doi.org/10.1029/ 2003JC001902

Son, T. P. H., van Lahn, V., Long, B. H., and Khin, L. V. 2005. Main structure of sea surface temperature (SST) in South China Sea from satellite data. Asian Conference on Remote Sensing (ACRS), 2005: 1-5.

Sun, C. 2017. Riverine influence on ocean color in the equatorial South China Sea. Continental Shelf Research, 143: 151-158.

Wang, D., Wang, H., Li, M., Liu, G., and Wu, X. 2013. Role of Ekman transport versus Ekman pumping in driving summer upwelling in the South China Sea. Journal of Ocean University of China, 12(3): 355–365. https://doi.org/10.1007/s11802-013-1904-7

Wyrtki, K. 1961. Physical oceanography of the Southeast Asian waters (Vol. 2). University of California, Scripps Institution of Oceanography. https://doi.org/10.1017/S0025315400054370

Xie, S.-P., Xie, Q., Wang, D., and Liu, W. T. 2003. Summer upwelling in the South China Sea and its role in regional climate variations. Journal of Geophysical Research, 108(C8), 3261. https://doi.org/10.1029/2003JC001867

Yan, Y., Ling, Z., and Chen, C. 2015. Winter coastal upwelling off northwest Borneo in the South China Sea. Acta Oceanologica Sinica, 34(1): 3–10. https://doi.org/ 10.1007/s13131-015-0590-2

Zainol, Z., and Akhir, M. F. 2016. Coastal upwelling at Terengganu and Pahang coastal waters: Interaction of hydrography, current circulation and phytoplankton biomass. Jurnal Teknologi, 78(8): 11–27. https://doi.org/10.11113/jt.v78.7402